Biomedical Signal Processing and Control 86 (2023) 105168

Contents lists available at ScienceDirect

Biomedical Signal Processing and Control

journal homepage: www.elsevier.com/locate/bspc

Imaging photoplethysmography quantifies endothelial dysfunction in patients with risk factors for cardiovascular complications

Natalia P. Podolyan [a], Irina A. Mizeva [b], Oleg V. Mamontov [a,c], Valeriy V. Zaytsev [a,c], Anzhelika V. Belaventseva [a], Anastasiia V. Sakovskaia [a,d], Roman V. Romashko [a], Alexei A. Kamshilin [a,*]

[a] Laboratory of New Functional Materials for Photonics, Institute of Automation and Control Processes of Far East Branch of the Russian Academy of Sciences, Vladivostok, Russia
[b] Institute of Continuous Media Mechanics of Ural Branch of the Russian Academy of Sciences, Perm, Russia
[c] Department of Circulation Physiology, Almazov National Medical Research Centre, Saint Petersburg, Russia
[d] Institute of Therapy and Instrumental Diagnostics, Pacific State Medical University, Vladivostok, Russia

ARTICLE INFO

Keywords:
Risk factors
Endothelial dysfunction
Imaging photoplethysmography
Local hyperemia
Vascular tone oscillations

ABSTRACT

The endothelium plays an important role in the pathogenesis of cardiovascular pathology, so that revealing its dysfunction can predict outcomes of the disease. However, the correct assessment of the endothelial function remains an unsolved problem. Registration of endothelium dependent vasodilation in response to nitric oxide synthesis using available noninvasive technologies does not show sufficient specificity and sensitivity, although it helps to detect its differences in population studies. In this pilot study, we compared the dynamics of microcirculation of the forearm skin and its spectral parameters during mild heating (up to 42 °C) between groups of smokers (n = 17) and non-smokers (n = 21) using imaging photoplethysmography synchronized with electrocardiography. The study included healthy men with similar anthropometric characteristics at the age of 51 ± 8 years and 48 ± 13 years, respectively. During the comparative analysis, no intergroup difference was found in the perfusion increase in either the axon- or endothelial-related phases of the reaction to local hyperemia. However, it was revealed that the power spectral density in the frequency band 0.01–0.02 Hz is significantly smaller in smokers than in non-smokers only during the phase of endothelium induced vasodilation: 4.0 ± 1.1 versus 5.3 ± 1.2 rel.un., respectively ($P = 0.005$). At the same time, no difference in the spectral power in the same band was observed during the axon-mediated phase, thus indicating high sensitivity and selectivity for assessment of the nitric oxide dependent vascular reactivity. The obtained results can be used for noninvasive evaluation of other cardiometabolic risk factors for early prediction and timely prevention of adverse outcomes by optimizing and intensifying treatment.

1. Introduction

Functional abnormalities of microvessels are commonly observed in patients with cardiovascular risk factors such as hypertension [1,2], diabetes mellitus [3,4], dyslipidemia [5], smoking [6,7], and obesity [8]. Alterations in small resistance arteries occur very early in hypertension, increasing vascular resistance and risk of hypertension complications, potentially leading to a worse prognosis [9]. Exposure to cardiovascular risk factors accompanies by endothelial dysfunction which manifests itself as insufficient endothelium-dependent vasodilation in response to vasoactive stimuli [9–11]. Endothelial dysfunction is documented in most conditions associated with cardiovascular pathologies, thereby allowing it to be considered as an early marker of future cardiovascular events [12,13]. Therefore, evaluation of endothelial dysfunction may provide clinically relevant information about cardiovascular risk with possible optimization of the treatment [14].

Non-invasive assessing of the functional changes provided by small resistance arteries in humans is a non-trivial and difficult task. Several methods were proposed to assess either anatomic features or the

* Corresponding author.
E-mail addresses: podolian@iacp.dvo.ru (N.P. Podolyan), mizeva@icmm.ru (I.A. Mizeva), ange202@mail.ru (A.V. Belaventseva), sakovska86@mail.ru (A.V. Sakovskaia), romashko@iacp.dvo.ru (R.V. Romashko), alexei.kamshilin@yandex.ru (A.A. Kamshilin).

https://doi.org/10.1016/j.bspc.2023.105168
Received 18 March 2023; Received in revised form 24 May 2023; Accepted 9 June 2023
Available online 15 June 2023

response of peripheral blood vessels, which can be divided into distal and proximal, depending on the region in which the blood flow is assessed, or mainly anatomical and functional, depending on the nature of the studied indicators. A typical example of an anatomical approach is a nailfold videocapillaroscopy with post-occlusive reactive hyperemia, which allows us to assess a number of parameters indicating microcirculation violation: changes in the number of functioning capillaries, the rate of erythrocytes after removal of occlusion, the ratio of the diameter of arterial and venous vessels, the thickness of the walls of arterioles and some others [15,16]. However, the use of different parameters to estimate microvascular alterations has led to inconsistent results on nailfold videocapillaroscopy capacity to provide reliable estimates of cardiometabolic risk [14,17].

The anatomic approach also includes the assessment of the anatomical features of retinal vessels, which has been used for a long time in clinical studies for the staging of hypertension. However, the technique is not enough sensitive and specific to detect early vascular abnormalities and does not allow performing a functional assessment of the endothelium. Nevertheless, the technology development and the recent use of adaptive optical ophthalmoscopy has made it possible to improve diagnostic indicators by objectifying visual assessment, which is achieved due to the possibility of measuring the wall-to-lumen ratio of retinal arterioles with diameters of 50 to 150 μm in-vivo [18,19]. Unfortunately, there are still no studies that would objectively show the prognostic value of the identified parameters in the early stages of hypertension. An important deterrent to this technology is very expensive equipment and requirement to highly qualified specialists.

Evaluation of the function of the endothelium of distal vessels is implemented in the technology of endothelial tonometry of peripheral arteries (EndoPat) [20–22]. This is one of the most widely used methods for assessing microvascular function, during which the reactivity of blood vessels is evaluated in response to the effect of under-oxidized products on the endothelium and, to a lesser extent, on the muscle wall, the response of which provides vasodilation of microvessels, thus increasing the volumetric blood flow rate. The main disadvantage of the method is its high cost, as well as some discrepancies in its prognostic value. In addition, there are still no significant population studies confirming the efficacy of the EndoPat [11]. It is also assumed that the increase in the amplitude of the pulse wave during reactive hyperemia, along with endothelium-dependent, may also include endothelium-independent vasodilation due to the influence of under-oxidized products directly on muscle cells [14].

Dynamic response of the endothelium to shear stresses causing vasodilatation can be assessed by measuring the diameter of the brachial (or radial) artery with high-resolution ultrasound [23,24]. The main disadvantages of this most common technique are a strong dependence on the operator, which makes it difficult to compare the results of different laboratories and significant variations in parameters measured on different days [25].

Laser Doppler flowmetry (LDF) is the most widely used functional approach to study the vascular endothelium, including measurements of the response of blood flow to various stimuli such as reactive hyperemia [26], physical exercise [27], and local heating [28–30], the latter being more frequently applied. It should be pointed out that vulnerability of LDF is in the physical principle behind this method: the measured signal is caused by a shift in the Doppler frequency, which is determined not only by the motion of red blood cells, but also by many other movements either unrelated or indirectly related to blood flow [31], which significantly reduces the reliability of the interpretation of the data obtained.

There is another optical technique, laser speckle contrast imaging (LSCI), which is also widely used for microcirculation studies [32,33]. LSCI is a camera-based technique allowing full-field blood flow visualization with high spatial resolution [34]. Although speckle contrast values are indicative of the level of motion in the sample, they are not directly proportional to the either velocity of red blood cells or blood flow [35]. Since dynamic speckles are very sensitive to any variations of the biological tissue (such as pulsations of arteries' walls or mussels contractions), and these changes which are aggravated by multiple light scattering, the results of the LSCI technique are ambiguous in interpretation [36].

Recently another optical modality, photoplethysmography, attracted attention of the researchers from different groups as a technique capable of quantifying activity of the autonomous nervous system by assessing changes in blood flow parameters [37–42]. Innovative modification of this technique, imaging photoplethysmography (iPPG), enables contactless extraction of physiological information about functioning of the cardiovascular system using conventional cameras [38,39,41]. In particular, feasibility of iPPG system to evaluate the vascular response to the cold stress [41], heat [43], and cognitive [39] tests have been demonstrated. Moreover, it was recently shown that iPPG allows for the assessment of the spatial distribution of the arterial tone [44] and vascular resistance [45]. More recent comparative studies of the response to physiological stimuli by iPPG and LSCI [39,46] confirmed that variations in the signal obtained by both techniques are determined by cutaneous blood flow whereas measurements of perfusion using iPPG was shown to be robust [46].

Functional tests are utilized for microvascular assessment. Local mild heating of skin to about 42 °C (thermal hyperemia) is known to induce significant relaxation of the microvascular smooth muscle cells due to the endothelial release of the nitric oxide (NO) and, thus, to achieve the local hyperperfusion [30,47]. Blood flow response has repeatable biphasic shape: first, blood flow rapidly increases, then reaches the local peak, and decreases down to the local nadir followed by a recurring increase, turning into a long plateau after 20–30 min of heating [47–49]. The peak in the first phase is mainly caused by the axon reflex of local sensory nerves [50]. It was shown that a greater contribution to the axon reflex is made by the cation-selective ion channel of vanilloid type 1 (TRPV1), mainly localized on sensitive nerves [51]. In the second phase, the increase in blood flow is caused by the humoral response, mainly associated with endothelial factors, among which NO accounts for about two-thirds of the contribution [50]. The endothelial hyperpolarizing factor, part of the action of which depends on epoxyeicosatrienoic acid, is also involved in the formation of the second phase of the blood flow response to local heating [52]. Therefore, local thermal hyperemia provides an opportunity for instrumental assessment of global endothelial dysfunction [49,53].

All of the above features of thermal hyperemia were experimentally identified using an LDF probe [28], which evaluates blood flow at a single point in contact with the skin. Low reproducibility of the LDF method is often associated with variations in the site of measurement, while the pressure of the probe on the skin is not controlled [48,54]. To overcome the limitations of LDF, we recently proposed using iPPG for assessing reaction on the local heating as a technique capable of estimating blood flow parameters over an extended skin area [55]. This technique is featured by accurate control of the parameters affecting microcirculation during the prolonged study. Despite the fact that LDF and iPPG signals related to blood flow parameters in fundamentally different way, it was found that the response to local hyperemia is similar and has a biphasic character with multiple increase of the signal [55].

Evaluation of endothelial function is an important way to predict the development and course of the disease in individuals with various risk factors of the cardiovascular system [56]. One of the risk factors determining the prognosis is tobacco smoking because it leads to a pathological change in the vascular endothelium due to a decrease in the activity and bioavailability of NO [7,57,58]. The interaction of NO with free radicals contained in tobacco smoke causes a change in biosynthesis and a decrease in NO activity. These disorders subsequently lead to endothelial dysfunction, which is expressed in a decrease in its vasodilating, antithrombotic, anti-inflammatory and antioxidant properties. However, as further studies have shown, there are other reasons for the influence of smoking on the prognosis. On the one hand, smoking is

associated with a violation of endothelium-dependent vasodilation, even after one smoked cigarette [59]. On the other hand, smokers have an increased risk of diseases of the cardiovascular system not only associated with atherosclerosis, but also the progression of hypertension, thromboembolism and possibly atrial fibrillation [60], the development of which may also be mediated by endothelial dysfunction.

There were quite a few studies devoted to noninvasive assessment of smoker's blood microcirculation [61–65]. Recent comparative study of blood circulation between smoking and non-smoking subjects using a wearable LDF sensor did not reveal significant difference in endothelial oscillations between these groups [65]. In contrast, basing on our more recent study of the response of blood flow parameters to moderate local heating using iPPG [55], we suggest that the latter method is more advantageous for reliable non-invasive assessment of endothelial dysfunction. The present study is aimed at comparing the parameters of the blood flow response to local forearm heating in smokers and non-smokers by means of the iPPG system.

The rest of the paper is organized as follows. In the Section 2, we describe material and methods of the study, namely groups of subjects, study protocol, measuring system, data processing, and statistical methods. The results of our study are presented in the Section 3. Sections 4 and 5 include discussion and conclusions of the results obtained.

2. Materials and methods

2.1. Participants and study protocol

The present study was carried out in the Private healthcare institution "Central clinical hospital "RZD-Medicine" Vladivostok" and in the Institute of Automation and Control Processes of Far East Branch of the Russian Academy of Sciences in accordance with ethical standards presented in the 2013 Declaration of Helsinki. All subjects signed the written Informed Consent Form enclosed in the study protocol approved by the Interdisciplinary Ethics Committee of the Pacific State Medical University, Vladivostok, Russia, decision No. 10 of 20 June 2021. All 38 participants in this pilot study were men. The mean age of subjects from the group of smokers (n = 17) was 51 ± 8 years. The average smoking experience was 28 years, and everyone was smoking at least one tobacco cigarette in 12 h. The control group (n = 21) consisted of non-smoking subjects of comparable age (48 ± 13 years). In addition, the subjects of both groups had comparable blood pressure levels and body mass index at the time of the study, the data are presented in Table 1. The exclusion criteria were as following: presence of cardiovascular disease risk factor such as hyperlipidemia, diabetes, and hypertension; severe concomitant systemic diseases, including respiratory, hepatic and renal failure, and skin diseases; history of drug dependence or persistent alcohol consumption.

Measuring sessions were carried out in a specially prepared darkened room with appropriate sanitary conditions and a temperature of 23 ± 1 °C. At least two hours before the study, the subjects did not take drugs that affect the vasomotor properties of blood vessels, abstained from eating and a large volume of liquid (including tea and coffee), were not exposed to physical exertion, and did not smoke. The subject was invited into the room fifteen minutes before the measuring session to adapt to the conditions of measurements. During this time, his well-being was clarified, anamnesis was collected, anthropometric parameters were determined, arterial pressure and pulse rate were measured. The subject was offered to take a comfortable position sitting on a chair, leaning back, with his legs uncrossed and breathing normally. His right hand was comfortably positioned on the measuring support at the heart level. Assessment of the blood flow response to local heating was carried out in three stages. At first, a video of a skin area under study was recorded continuously and synchronously for one minute together with an electrocardiogram (ECG) and skin temperature (baseline recording). Then, the region under study was heated up to 40 – 42 °C at a heating rate of about 3.5° C per minute to avoid painful sensations [66]. The achieved skin temperature was maintained for 15 min. At the third stage, the heating module was turned off, and the skin temperature relaxed naturally. At all stages of the local heating test, the video, ECG, and temperature were continuously recorded.

Table 1
Characteristics of subjects in the groups under study.

	Group of smokers (n = 17)	Control group (n = 21)	Significance of differences
Age (years)	51 ± 8	48 ± 13	P = 0.49
Male/Female	17/0	21/0	
Smoking experience (years)	28 ± 12	0	
Body mass index (kg/m^2)	29 ± 4	27 ± 3	P = 0.09
Systolic blood pressure (mmHg)	131 ± 12	125 ± 9	P = 0.11
Diastolic blood pressure (mmHg)	82 ± 7	83 ± 8	P = 0.88

Data are expressed as mean ± standard deviation.

2.2. Measuring system

Our custom-made iPPG system involved synchronous acquisition of video frames, ECG, and skin temperature signals. The layout of the system is shown in Fig. 1, while all components were described in details before [55]. Briefly, a glass plate sizing 70 × 20 × 2 mm^3 with a transparent conductive layer (a heating device) was placed on the outer side of subject's forearm providing local skin heating. The heating device and the skin under it were evenly illuminated by 250 light-emitting diodes (LEDs) arranged in four concentric rings around the camera lens and operated at the wavelength of 530 ± 25 nm (green light). Images in reflected light were recorded by a monochrome 8-bit digital camera (model "UI-3060CP-M−GL," Imaging Development Systems GmbH, Obersulm, Germany) mounted together with the LED-illuminator. The video recording of the heated area was made at the rate of 36 frames per second with a resolution of 340 by 286 pixels. The video data were

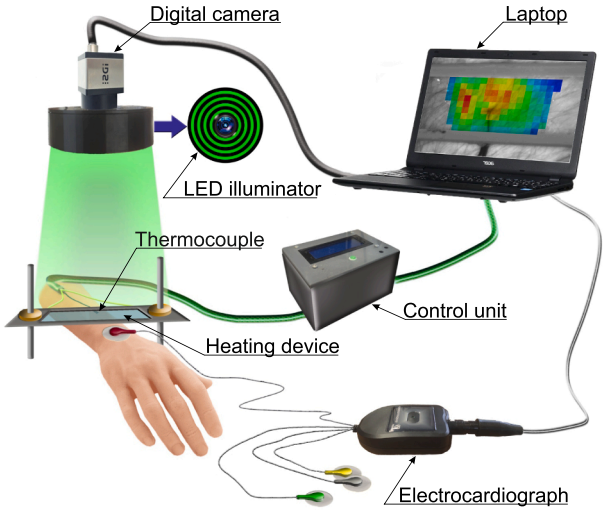

Fig. 1. Schematic of the experimental setup. The measuring system includes a ring-shaped light-emitting-diodes (LEDs) illuminator providing green light (wavelength 530 ± 25 nm) for uniform illumination of an area under study, digital monochrome camera equipped with a 12-mm-focus length, a transparent heating device controlled by control unit and an electrocardiograph. The data is recorded synchronously and written to the computer's memory. The laptop screen displays an example of a perfusion map superimposed on an actual image of the area under study.

transferred to a personal computer and recorded on a solid-state hard disk. A digital electrocardiograph (model "KAP-01-Kardiotekhnika-EKG," Incart Ltd., Saint Petersburg, Russia) operating at the sampling rate of 1 kHz was used to record ECG in two leads. Recording of video frames and ECG were synchronized with accuracy of 1 ms.

Note that the pressure of the heating plate on the skin was assessed for each subject and did not exceed 15 mmHg. Liquid petroleum jelly was applied between the heating plate and the skin to ensure heat transfer from the heating device. Skin temperature was measured synchronously with the video and ECG recordings by means of K-type thermocouple located between the heating plate and the skin. The control unit transmitted temperature readings with the rate of 5 Hz to a personal computer via a serial port, and also controlled the voltage applied to the heating device in accordance with the pre-recorded program.

2.3. Data processing

The recorded data were processed offline by using an algorithm described in details in our previous paper [55]. Briefly, it includes the following steps. At the first step, a digital image stabilization algorithm is utilized to minimize the impact of motion artifacts. Since different areas of the skin can shift in different directions, the entire image frame is divided into segments, followed by independent compensation for the displacement of each segment.

At the second step, the part of the image located inside the visible boundary of the liquid oiling is divided into adjacent regions of interest (ROI) with a size of 15 × 15 pixels, which is about 4 mm^2 on the forearm. A iPPG-waveform is calculated as a frame-by-frame evolution of the average pixel value in each ROI. Pulsation amplitude at the heart rate is calculated as the difference between the maximum and minimum value of the iPPG-waveform in every cardiac cycle, the beginning and end of which were determined by R-peaks of a synchronously recorded ECG. Then the ratio of this amplitude and the mean value of the iPPG-waveform in each ROI is calculated to compensate for possible unevenness of tissue illumination. This ratio is denoted here as amplitude of pulsatile component (APC). In this way, we estimate the variations in time (once per cardiac cycle) of the APC parameter, which, as is known, reflects the perfusion of the arteries nearby the measurement site [44]. The APC is assessed in each ROI. As it was found in our preliminary study, perfusion has inhomogeneous spatial distribution, which varies from one subject to another, but for every subject the distribution remains unchanged during the local heating test [55]. To compensate for the difference in spatial distributions among the subjects, the APC is mapped over the examined area using the algorithm described in detail earlier [55,67], a half of the ROIs with higher APC is selected, and the APC is averaged over the selected ROIs to assess the mean perfusion dynamics. An example of the mean perfusion evolution during the heating test is shown in Fig. 2A. As seen in this graph, the perfusion response to local heating is two-phase: an increase in skin temperature leads to a multifold increase in APC, followed by a local nadir with subsequent increase turning into prolonged hyperemia. This biphasic type of the perfusion dynamics corresponds to that usually observed in a local heating test measured by LDF [68].

At the third step, the averaged dynamics of the perfusion variations in response to local heating is quantified. A perfusion gain factor (K_{max}) is defined as the ratio of the APC parameter at the peak of the first phase to the average APC value in the baseline. An integral response of the perfusion to heating during the first phase is calculated as the area under the APC curve between the moment of switching on the heater and the nadir point (S_1, shaded with yellow in Fig. 2A). An integral response during the second phase is evaluated as the area under the APC curve during 22 min from the nadir (S_2, shaded with lilac in Fig. 2A).

At the fourth step, a spectral analysis of the measured perfusion response was performed using either Fourier or wavelet transfers. In the latter case, we use one of the most popular wavelets – the Morlet wavelet, defined as

$$\psi(t) = e^{2\pi i t} e^{-t^2/(2\sigma^2)}. \tag{1}$$

Here t is time, and the parameter σ describes the length of the analyzing function, for $\sigma \to \infty$ wavelet transform approaches to the Fourier transform. In this study we use $\sigma = 1.7$. The continuous wavelet transforms of the signal $APC(t)$ are defined as

$$W(\nu, t) = \sqrt{\nu} \int_{-\infty}^{\infty} APC(t) \psi^*(\nu(t-\tau)) dt \tag{2}$$

where * means the complex conjugation, ν is the frequency, τ is the time shift. Integrating the power over the time period T gives the global wavelet spectrum

$$M(\nu) = \frac{1}{T} \int_0^T W(\nu, t)^2 dt \tag{3}$$

The wavelet spectrum $M(\nu)$ in Eq. (3) repeats the main features of the Fourier spectrum. The blue curve in Fig. 2B shows the Fourier spectrum for the second phase of the perfusion response to local heating (from the nadir point to 31th minute, Fig. 2A). To calculate the wavelet spectrum, we split the frequency range from 0.01 to 0.6 Hz into 50 frequency bands. The respective wavelet spectrum averaged over the same phase of the response is shown in Fig. 2B by the orange solid line. It is seen that the wavelet spectrum is a smoothed version of the Fourier spectrum [69], which makes it possible to more reliably identify the main features of short and noisy signals.

At the final step, we compared the averaged dynamics and power spectral density of perfusion responses to local heating among different subjects separately for the response during the first (between the heating start and nadir) and second (between the nadir and 31-th minute) phases. Since the level of perfusion varies greatly from one subject to another, the comparison was carried out using spectral power in the

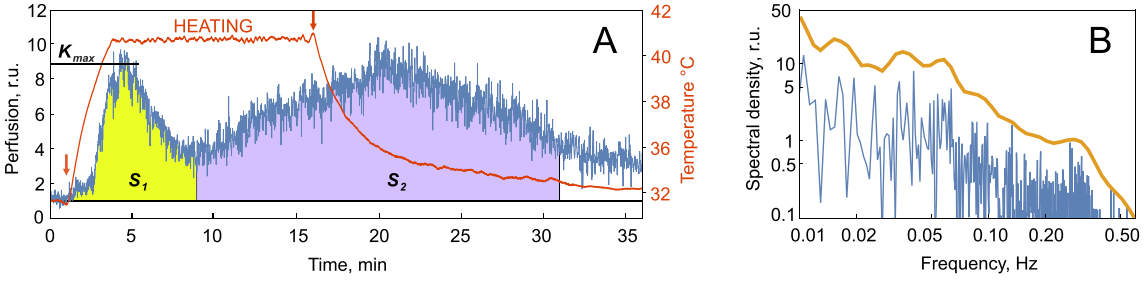

Fig. 2. An example of the perfusion dynamics during the heating test and its normalized spectra. A: Perfusion evolution for one of the smokers (blue line) and dynamics of his skin temperature (red line with arrows showing the start and end of heating). Yellow-shaded and lilac shaded segments indicate the first and second vasodilation phases, respectively. K_{max} - a perfusion gain factor; S_1 - an integral response of the perfusion to heating during the first phase; S_2 - an integral response during the second phase. B: Fourier (blue line) and wavelet normalized spectra (orange thick line), calculated for the second phase of the perfusion response.

bands normalized to the total spectral power for each subject.

2.4. Statistical analysis

The study used methods of non-parametric statistics. To test the hypothesis of the reliability of differences in independent variables, the Mann-Whitney U test was used. A 95% confidence interval was used. The level of significance of all of the statistical indicators is $P < 0.05$, unless otherwise indicated. The data are expressed as mean ± standard deviation (SD). Statistical analysis of the data was also performed in the Mathematica 10.3 (Wolfram research, USA).

3. Results

In most of the participants of our study, the perfusion response to local heating of the forearm skin manifests itself in the form of a two-phase curve shown in Fig. 2A with a clearly defined nadir point. More examples of the response curve can be seen in our recent paper [55]. Perfusion gain factor assessed in the peak of the first phase (K_{max}) turned out to vary greatly both in the group of smokers (from 3.2 to 14) and control (from 3.7 to 13.2). No statistically significant difference in this parameter was found between smokers and non-smokers (see Table 2). An even higher variability of the integral parameters (S_1 and S_2) of the perfusion increase was found in each response phase in both smokers and non-smokers. The median [minimal - maximal] S_1 during the response mediated by the axon reflex was 33.2 [9.6 – 64.3] and 37.6 [12.0 – 70.9] for smokers and control, respectively, while in the secondary phase S_2 was 113.2 [55.1 – 316.4] and 122.9 [23.8 – 238.0] for smokers and control, respectively. Therefore, comparative analysis of the averaged dynamics of perfusion did not reveal statistically significant differences in vasodilation between the control and smoking groups in any of the phases of the response to heating (see Table 2).

However, spectral analysis of APC dynamics during skin heating revealed significant intergroup differences in the reaction of the forearm microcirculation in response to local heating associated with endothelial function. The APC normalized wavelet spectra for smokers (orange boxes) and control (blue boxes) had been calculated during vasodilation mediated by the axon-reflex (first phase) and endothelium dependent vasodilation (second phase) and presented in Fig. 3A and Fig. 3C, respectively. As one can see, in different spectral bands, the ratio of the spectral density of perfusion oscillations between groups of smokers and non-smokers is different. No statistically significant difference was found in any of the spectral ranges when comparing the spectra averaged over each of the ranges during the vasodilation mediated by the axon reflex (Fig. 3A). For example, the boxplot of average spectral density in the endothelial frequency band (Fig. 3B) shows insignificant difference between the groups during the first phase of the response: $P = 0.2$. However, when comparing the spectral density of oscillations averaged over the endothelial frequency band during the second phase of the response (Fig. 3D), it was revealed that these oscillations in smokers are significantly lower than in non-smokers, $P = 0.005$.

Table 2
Relative perfusion parameters in the axon- and endothelium-related phases of vasodilation.

	Group of smokers ($n = 17$)	Control group ($n = 21$)	Significance of differences
Perfusion gain factor,K_{max}	7.8 ± 2.7	8.1 ± 2.5	$P = 0.67$
Integral increase of perfusion during the first phase, S_1, rel. un.	34 ± 17	39 ± 17	$P = 0.40$
Integral increase of perfusion during the second phase, S_2, rel. un.	121 ± 59	126 ± 52	$P = 0.79$
Endothelial oscillations during the first phase, rel. un.	4.0 ± 1.5	4.7 ± 1.5	$P = 0.2$
Endothelial oscillations during the second phase, rel. un.	4.0 ± 1.1	5.3 ± 1.2	$P = 0.005$

Data are expressed as mean ± standard deviation.

4. Discussion

In this study, we have utilized innovative iPPG system together with the protocol with local hyperemia to reveal endothelial function in patients with cardiovascular risk. The system combines continuous video recording of the heating region under green illumination synchronously with the ECG recording. Correlation analysis of iPPG and ECG signals allows us to reliably measure the APC parameter related to the perfusion of the studied region against the background of unavoidable motion artifacts [44,67]. Distinctive biphasic perfusion response to local heating (similar to previously detected LDF [29,47]) was found in all 38 subjects. The spectral analysis of the perfusion response revealed a significantly reduced energy of endothelial oscillations (0.01 – 0.02 Hz) in the group of smokers in the second phase, whereas no intergroup difference in this spectral band was found in the first phase. Considering that it is the second phase of the vasodilatory response to heating that is mainly associated with endothelial factors [50,70], the proposed method has demonstrated high sensitivity and selectivity of quantitative assessment of endothelial function. Unlike in spectral parameters, no statistically significant intergroup differences were revealed in any amplitude characteristic of the response. The latter can be due to large variability of the perfusion response among the subjects. Our pilot study has demonstrated for the first time the possibility of noninvasive assessment of endothelial function by the iPPG technique. The limitation of our study is that only men participated in it.

It is worth noting that here we use the same approach to spectral analysis of the data as in the case of LDF [65]. Therefore, we can focus on at least two main factors determining the advantages of iPPG over LDF in solving the problem of noninvasive evaluation of endothelial function.

1. The most important is the fundamental difference in the blood flow parameters measured by these two methods. If the LDF signal is a nonlinear function of the averaged velocity of erythrocytes moving in vessels, then in the iPPG method, the measured parameter APC is proportional to the amplitude of pulsations of arterial vessels supplying the measured area of the skin. In our iPPG system we use green light, which acquires the greatest modulation at the heart rate been interacting with biological tissue containing blood vessels, while the depth of its penetration into the skin does not exceed 0.5 mm. Despite the widespread use and acceptability of iPPG, the origin of the iPPG signal is a subject of continuing debate [71–73]. According to a recently proposed alternative model of iPPG [72], its waveform is derived from mechanical compression / relaxation of the dermis capillaries due to pulsations of nearby arteries and arterioles. Since the main cause of perfusion is a pulse-pressure wave originated from the heart, the dynamics of the normalized amplitude of arterial pulsations, APC parameter, reflects the changes in the tone of these vessels [44,74].
2. For a reliable assessment of low–frequency endothelial oscillations (0.01–0.02 Hz), continuous measurement of blood flow parameters is necessary for a long time (more than 15 min to measure at least 10 periods of endothelial oscillations) with mandatory stability of parameters that may affect blood flow during a local heating test. Moreover, the characteristic time of the development of the endothelium-dependent vasodilation is 10 min from the heater switching on. During the local heating test, contact of the heater with the skin is necessary for the efficient transfer of thermal energy. At the same time, it is well known that any contact with the skin causes changes in blood flow [72,75]. When using a fiber-optic LDF probe, the contact area is quite small and the pressure on the skin is difficult to control. In contrast, in our study, a heater of a larger area,

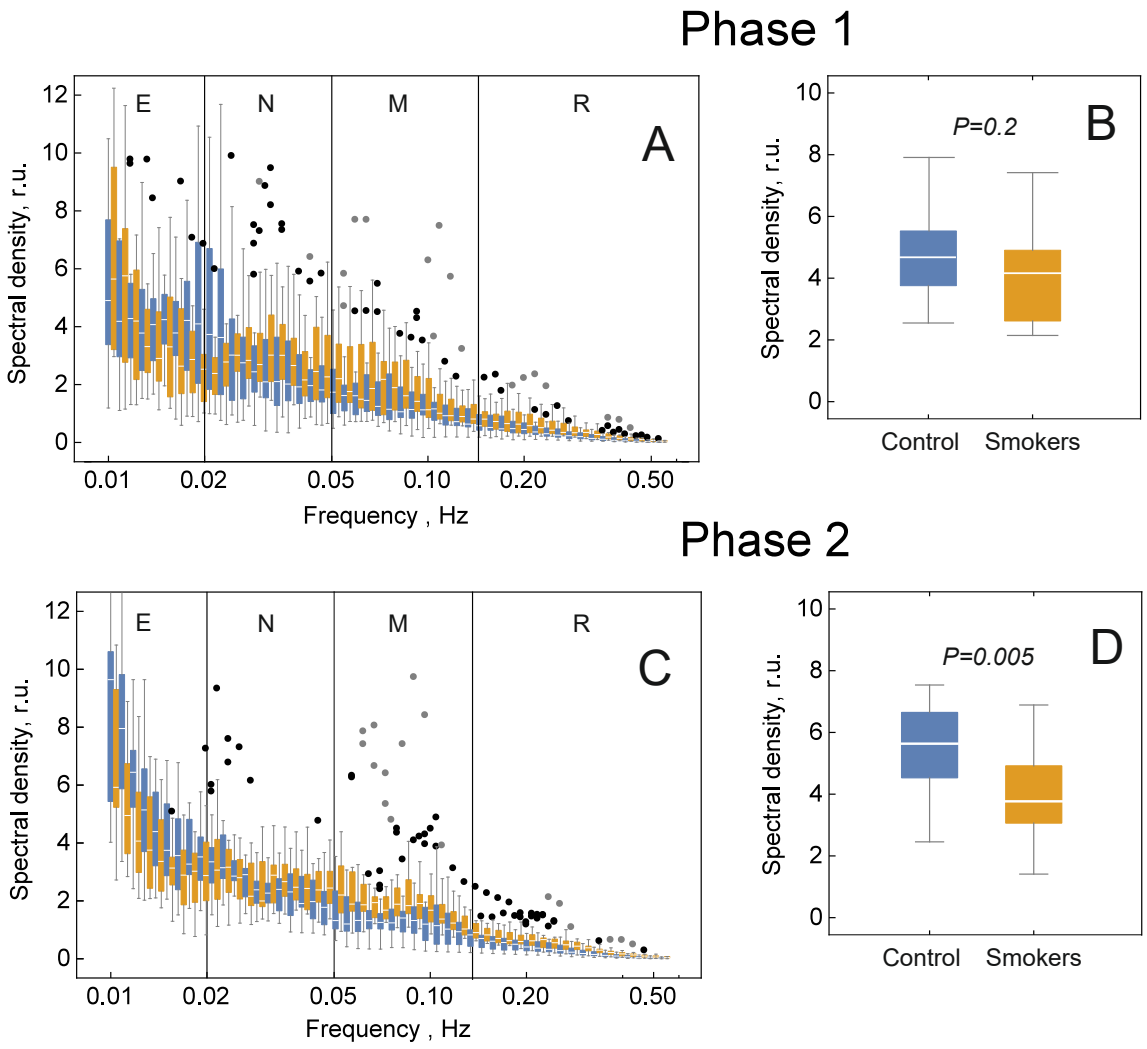

Fig. 3. Comparison of perfusion response spectra to local heating between the control group (blue rectangles) and smokers (orange rectangles). Diagrams of APC spectra assessed during the first phase of the response (vasodilation mediated by axon reflex) and during the second phase (endothelium induced dilation) are shown in the upper and lower parts, respectively. Panels A and C show box whisker diagrams for APC normalized spectral density. Vertical lines in these panels indicate endothelial (E), neurogenic (N), myogenic (M), and respiratory (R) frequency bands. B and D: spectral density averaged over the endothelial band (0.01–0.02 Hz).

separated from optical elements was used. This allowed us to reduce the pressure on the skin and control it during long-term measurements. In addition, simultaneous measurement of blood-flow parameters over a large area using iPPG system makes it possible to take into account the heterogeneity of the perfusion distribution caused by the peculiarities of the vascular morphology of each individual subject.

5. Conclusions

The differences we found in the vascular response to mild heating of the forearm skin during the phase of endothelium induced dilation show the possibilities of the technique for detecting the initial damaging effects of tobacco smoking at the level of the microcirculatory bed in the form of a decrease in NO-dependent vascular reactivity and indicates a high potential of the iPPG system for assessing endothelial function. Since smokers represent one of the groups of patients at risk of cardiovascular diseases, we believe that the proposed non-invasive method of selective assessment of endothelial function will allow to develop systems for early diagnosis of cardiovascular complications in other groups, as well.

CRediT authorship contribution statement

Natalia P. Podolyan: Conceptualization, Methodology, Formal analysis, Investigation, Data curation, Visualization, Writing – original draft. **Irina A. Mizeva:** Conceptualization, Formal analysis, Software, Writing – review & editing. **Oleg V. Mamontov:** Conceptualization, Methodology, Formal analysis, Writing – review & editing. **Valeriy V. Zaytsev:** Resources. **Anzhelika V. Belaventseva:** Investigation, Data curation, Visualization. **Anastasiia V. Sakovskaia:** Investigation, Resources. **Roman V. Romashko:** Supervision, Project administration. **Alexei A. Kamshilin:** Conceptualization, Methodology, Software, Data curation, Supervision, Writing – review & editing.

Declaration of Competing Interest

The authors declare that they have no known competing financial interests or personal relationships that could have appeared to influence the work reported in this paper.

Data availability

Data will be made available on request.

Acknowledgement

Fundings: The study was carried out with the financial support of the Russian Science Foundation (grant No. 21-15-00265) in terms of experiment planning, manufacturing and calibration of a laboratory installation, development of a data processing algorithm. Spectral data analysis was performed with the financial support of the Ministry of Education and Science of Russia (grant No. AAAA19-119012290101-5).

References

[1] M.J. Mulvany, C. Aalkjaer, Structure and function of small arteries, Physiol. Rev. 70 (1990) 921–961, https://doi.org/10.1152/physrev.1990.70.4.921.
[2] H. Brunner, J.R. Cockcroft, J. Deanfield, A. Donald, E. Ferrannini, J. Halcox, W. Kiowski, T.F. L??scher, G. Mancia, A. Natali, J.J. Oliver, A.C. Pessina, D. Rizzoni, G.P. Rossi, A. Salvetti, L.E. Spieker, S. Taddei, D.J. Webb, Endothelial function and dysfunction. Part II: Association with cardiovascular risk factors and diseases. A statement by the Working Group on Endothelins and Endothelial Factors of the European Society of Hypertension, J. Hypertens. 23 (2) (2005) 233–246.
[3] S. Mäkimattila, A. Virkamäki, P.-H. Groop, J. Cockcroft, T. Utriainen, J. Fagerudd, H. Yki-Järvinen, Chronic Hyperglycemia Impairs Endothelial Function and Insulin Sensitivity Via Different Mechanisms in Insulin-Dependent Diabetes Mellitus, Circulation 94 (1996) 1276–1282, https://doi.org/10.1161/01.CIR.94.6.1276.
[4] I. Schofield, R. Malik, A. Izzard, C. Austin, A. Heagerty, Vascular Structural and Functional Changes in Type 2 Diabetes Mellitus, Circulation 106 (2002) 3037–3043, https://doi.org/10.1161/01.CIR.0000041432.80615.A5.
[5] L.E. Spieker, I. Sudano, D. Hürlimann, P.G. Lerch, M.G. Lang, C. Binggeli, R. Corti, F. Ruschitzka, T.F. Lüscher, G. Noll, High-Density Lipoprotein Restores Endothelial Function in Hypercholesterolemic Men, Circulation 105 (2002) 1399–1402, https://doi.org/10.1161/01.CIR.0000013424.28206.8F.
[6] D.S. Celermajer, K.E. Sorensen, D. Georgakopoulos, C. Bull, O. Thomas, J. Robinson, J.E. Deanfield, Cigarette smoking is associated with dose-related and potentially reversible impairment of endothelium-dependent dilation in healthy young adults, Circulation 88 (1993) 2149–2155, https://doi.org/10.1161/01.CIR.88.5.2149.
[7] A. Virdis, C. Giannarelli, M.F. Neves, S. Taddei, L. Ghiadoni, Cigarette smoking and hypertension, Curr. Pharm. Des. 16 (2010) 2518–2525, https://doi.org/10.2174/138161210792062920.
[8] H.O. Steinberg, H. Chaker, R. Leaming, A. Johnson, G. Brechtel, A.D. Baron, Obesity/insulin resistance is associated with endothelial dysfunction. Implications for the syndrome of insulin resistance, J. Clin. Invest. 97 (1996) 2601–2610, https://doi.org/10.1172/JCI118709.
[9] E. Agabiti-Rosei, D. Rizzoni, Microvascular structure as a prognostically relevant endpoint, J. Hypertens. 35 (2017) 914–9212, https://doi.org/10.1097/HJH.0000000000001259.
[10] S. Masi, G. Georgiopoulos, M. Chiriacò, G. Grassi, G. Seravalle, C. Savoia, M. Volpe, S. Taddei, D. Rizzoni, A. Virdis, on behalf of the S.G. on M.M. of the I.S. of H. (SIIA), The importance of endothelial dysfunction in resistance artery remodelling and cardiovascular risk, Cardiovasc. Res. 116 (2020) 429–437, https://doi.org/10.1093/cvr/cvz096.
[11] E. Vizzardi, M. Gavazzoni, P. Della Pina, I. Bonadei, V. Regazzoni, E. Sciatti, E. Trichaki, R. Raddino, M. Metra, Noninvasive Assessment of Endothelial Function: The Classic Methods and the New Peripheral Arterial Tonometry, J. Investig. Med. 62 (2014) 856–864, https://doi.org/10.1097/JIM.0000000000000096.
[12] N.H. Buus, O.N. Mathiassen, M. Fenger-Grøn, M.N. Præstholm, I. Sihm, N.K. Thybo, A.P. Schroeder, K. Thygesen, C. Aalkjær, O.L. Pedersen, M.J. Mulvany, K. L. Christensen, Small artery structure during antihypertensive therapy is an independent predictor of cardiovascular events in essential hypertension, J. Hypertens. 31 (2013) 791–797, https://doi.org/10.1097/HJH.0b013e32835e215e.
[13] T.J. Anderson, M.D. Gerhard, I.T. Meredith, F. Charbonneau, D. Delagrange, M. A. Creager, A.P. Selwyn, P. Ganz, Systemic nature of endothelial dysfunction in atherosclerosis, Am. J. Cardiol. 75 (1995) 71B–74B, https://doi.org/10.1016/0002-9149(95)80017-M.
[14] D. Rizzoni, A. Mengozzi, S. Masi, C. Agabiti Rosei, C. De Ciuceis, A. Virdis, New Noninvasive Methods to Evaluate Microvascular Structure and Function, Hypertension 79 (2022) 874–886, https://doi.org/10.1161/HYPERTENSIONAHA.121.17954.
[15] C.L.C. Junqueira, M.E.C. Magalhães, A.A. Brandão, E. Ferreira, F.Z.G.A. Cyrino, P. A. Maranhão, M.D.G.C. Souza, D.A. Bottino, E. Bouskela, Microcirculation and biomarkers in patients with resistant or mild-to-moderate hypertension: a cross-sectional study, Hypertens. Res. 41 (7) (2018) 515–523, https://doi.org/10.1038/s41440-018-0043-3.
[16] A.D. Tarnoki, D.L. Tarnoki, G. Pucci, Early detection of microvascular dysfunction in hypertension: the holy grail of cardiovascular prevention and risk assessment? Hypertens. Res. 41 (2018) 780–782, https://doi.org/10.1038/s41440-018-0086-5.
[17] D. Paxton, J.D. Pauling, Does nailfold capillaroscopy help predict future outcomes in systemic sclerosis? A systematic literature review, Semin. Arthritis Rheum. 48 (2018) 482–494, https://doi.org/10.1016/j.semarthrit.2018.02.005.
[18] A. Gallo, T. Dietenbeck, A. Giron, M. Paques, N. Kachenoura, X. Girerd, Non-invasive evaluation of retinal vascular remodeling and hypertrophy in humans: intricate effect of ageing, blood pressure and glycaemia, Clin. Res. Cardiol. 110 (2021) 959–970, https://doi.org/10.1007/s00392-020-01680-3.
[19] E. Koch, D. Rosenbaum, A. Brolly, J.-A. Sahel, P. Chaumet-Riffaud, X. Girerd, F. Rossant, M. Paques, Morphometric analysis of small arteries in the human retina using adaptive optics imaging: relationship with blood pressure and focal vascular changes, J. Hypertens. 32 (2014) 890–898, https://doi.org/10.1097/HJH.0000000000000095.
[20] J.T. Kuvin, A.R. Patel, K.A. Sliney, N.G. Pandian, J. Sheffy, R.P. Schnall, R.H. Karas, J.E. Udelson, Assessment of peripheral vascular endothelial function with finger arterial pulse wave amplitude, Am. Heart J. 146 (2003) 168–174, https://doi.org/10.1016/S0002-8703(03)00094-2.
[21] S. Masi, D. Rizzoni, S. Taddei, R.J. Widmer, A.C. Montezano, T.F. Lüscher, E. L. Schiffrin, R.M. Touyz, F. Paneni, A. Lerman, G.A. Lanza, A. Virdis, Assessment and pathophysiology of microvascular disease: recent progress and clinical implications, Eur. Heart J. 42 (2021) 2590–2604, https://doi.org/10.1093/eurheartj/ehaa857.
[22] M. Jakubowski, A. Turek-Jakubowska, E. Szahidewicz-Krupska, K. Gawrys, J. Gawrys, A. Doroszko, Profiling the endothelial function using both peripheral artery tonometry (EndoPAT) and Laser Doppler Flowmetry (LD) - Complementary studies or waste of time? Microvasc. Res. 130 (2020), 104008 https://doi.org/10.1016/j.mvr.2020.104008.
[23] D.S. Celermajer, K.E. Sorensen, V.M. Gooch, D.J. Spiegelhalter, O.I. Miller, I. D. Sullivan, J.K. Lloyd, J.E. Deanfield, Non-invasive detection of endothelial dysfunction in children and adults at risk of atherosclerosis, Lancet 340 (1992) 1111–1115, https://doi.org/10.1016/0140-6736(92)93147-F.
[24] M.C. Corretti, T.J. Anderson, E.J. Benjamin, D. Celermajer, F. Charbonneau, M. A. Creager, J. Deanfield, H. Drexler, M. Gerhard-Herman, D. Herrington, P. Vallance, J. Vita, R. Vogel, Guidelines for the ultrasound assessment of endothelial-dependent flow-mediated vasodilation of the brachial artery, J. Am. Coll. Cardiol. 39 (2002) 257–265, https://doi.org/10.1016/S0735-1097(01)01746-6.
[25] J. Deanfield, A. Donald, C. Ferri, C. Giannattasio, J. Halcox, S. Halligan, A. Lerman, G. Mancia, J.J. Oliver, A.C. Pessina, D. Rizzoni, G.P. Rossi, A. Salvetti, E. L. Schiffrin, S. Taddei, D.J. Webb, Endothelial function and dysfunction. Part I: Methodological issues for assessment in the different vascular beds: A statement by the Working Group on Endothelin and Endothelial Factors of the European Society of Hypertension, J. Hypertens. 23 (2005) 7–17. https://journals.lww.com/jhypertension/Fulltext/2005/01000/Endothelial_function_and_dysfunction__Part_I_.4.aspx.
[26] V. Tóth-Szűki, F. Bari, F. Domoki, Stable laser-Doppler flow-motion patterns in the human cutaneous microcirculation: Implications for prospective geroscience studies, Physiol. Int. 107 (2020) 134–144, https://doi.org/10.1556/2060.2020.00013.
[27] G.J. Hodges, P. Klentrou, S.S. Cheung, B. Falk, Comparison of laser speckle contrast imaging and laser-Doppler fluxmetry in boys and men, Microvasc. Res. 128 (2020), 103927, https://doi.org/10.1016/j.mvr.2019.103927.
[28] C.T. Minson, L.T. Berry, M.J. Joyner, Nitric oxide and neurally mediated regulation of skin blood flow during local heating, J. Appl. Physiol. 91 (2001) 1619–1626, https://doi.org/10.1152/jappl.2001.91.4.1619.
[29] K.A. Roberts, T. van Gent, N.D. Hopkins, H. Jones, E.A. Dawson, R. Draijer, H. H. Carter, C.L. Atkinson, D.J. Green, D.H.J. Thijssen, D.A. Low, Reproducibility of four frequently used local heating protocols to assess cutaneous microvascular function, Microvasc. Res. 112 (2017) 65–71, https://doi.org/10.1016/j.mvr.2017.03.005.
[30] M. Sorelli, P. Francia, L. Bocchi, A. De Bellis, R. Anichini, Assessment of cutaneous microcirculation by laser Doppler flowmetry in type 1 diabetes, Microvasc. Res. 124 (2019) 91–96, https://doi.org/10.1016/j.mvr.2019.04.002.
[31] A.A. Kamshilin, O.V. Mamontov, Physiological origin of camera-based PPG imaging, in: W. Wang, X. Wang (Eds.), Contactless Vital Signs Monit, Academic Press, London, 2022, pp. 27–50, https://doi.org/10.1016/B978-0-12-822281-2.00010-X.
[32] K.R. Forrester, J. Tulip, C. Leonard, C. Stewart, R.C. Bray, A laser speckle imaging technique for measuring tissue perfusion, IEEE Trans. Biomed. Eng. 51 (2004) 2074–2084, https://doi.org/10.1109/TBME.2004.834259.
[33] M. Draijer, E. Hondebrink, T. van Leeuwen, W. Steenbergen, Review of laser speckle contrast techniques for visualizing tissue perfusion, Lasers Med. Sci. 24 (2009) 639–651, https://doi.org/10.1007/s10103-008-0626-3.
[34] S.M.S. Kazmi, L.M. Richards, C.J. Schrandt, M.A. Davis, A.K. Dunn, Expanding applications, accuracy, and interpretation of laser speckle contrast imaging of cerebral blood flow, J. Cereb. Blood Flow Metab. 35 (2015) 1076–1084, https://doi.org/10.1038/jcbfm.2015.84.
[35] A.K. Dunn, Laser speckle contrast imaging of cerebral blood flow, Ann. Biomed. Eng. 40 (2012) 367–377, https://doi.org/10.1007/s10439-011-0469-0.
[36] S.M.S. Kazmi, E. Faraji, M.A. Davis, Y.-Y. Huang, X. Zhang, A.K. Dunn, Flux or speed? Examining speckle contrast imaging of vascular flows, Biomed, Opt. Express. 6 (2018) 2588–2608, https://doi.org/10.1364/BOE.6.002588.
[37] K. Budidha, P.A. Kyriacou, Photoplethysmography for quantitative assessment of sympathetic nerve activity (SNA) during cold stress, Front. Physiol. 9 (2019) 1863, https://doi.org/10.3389/fphys.2018.01863.
[38] O.V. Mamontov, T.V. Krasnikova, M.A. Volynsky, N.A. Anokhina, E.V. Shlyakhto, A.A. Kamshilin, Novel instrumental markers of proximal scleroderma provided by imaging photoplethysmography, Physiol. Meas. 41 (2020) 44004, https://doi.org/10.1088/1361-6579/ab807c.
[39] S. Rasche, R. Huhle, E. Junghans, M.G. de Abreu, Y. Ling, A. Trumpp, S. Zaunseder, Association of remote imaging photoplethysmography and cutaneous perfusion in

volunteers, Sci. Rep. 10 (2020) 16464, https://doi.org/10.1038/s41598-020-73531-0.
[40] D. Lapitan, D. Rogatkin, Optical incoherent technique for noninvasive assessment of blood flow in tissues: Theoretical model and experimental study, J. Biophotonics. 14 (2021) e202000459.
[41] S. Borik, S. Lyra, V. Perlitz, M. Keller, S. Leonhardt, V. Blazek, On the spatial phase distribution of cutaneous low-frequency perfusion oscillations, Sci. Rep. 12 (2022) 5997, https://doi.org/10.1038/s41598-022-09762-0.
[42] I.A. Mizeva, C. Di Maria, P. Frick, S. Podtaev, J. Allen, Quantifying the correlation between photoplethysmography and laser Doppler flowmetry microvascular low-frequency oscillations, J. Biomed. Opt. 20 (2015) 37007, https://doi.org/10.1117/1.JBO.20.3.037007.
[43] M.A. Volynsky, N.B. Margaryants, O.V. Mamontov, A.A. Kamshilin, Contactless monitoring of microcirculation reaction on local temperature changes, Appl. Sci. 9 (2019) 4947, https://doi.org/10.3390/app9224947.
[44] O.A. Lyubashina, O.V. Mamontov, M.A. Volynsky, V.V. Zaytsev, A.A. Kamshilin, Contactless assessment of cerebral autoregulation by photoplethysmographic imaging at green illumination, Front. Neurosci. 13 (2019) 1235, https://doi.org/10.3389/fnins.2019.01235.
[45] M.A. Volynsky, O.V. Mamontov, A.V. Osipchuk, V.V. Zaytsev, A.Y. Sokolov, A. A. Kamshilin, Study of cerebrovascular reactivity to hypercapnia by imaging photoplethysmography to develop a method for intraoperative assessment of the brain functional reserve, Biomed. Opt. Express. 13 (2022) 184–196, https://doi.org/10.1364/BOE.443477.
[46] D. Allan, N. Chokalingam, R. Naemi, Validation of a non-invasive imaging photoplethysmography device to assess plantar skin perfusion, a comparison with laser speckle contrast analysis, J. Med. Eng. Technol. 45 (2021) 170–176, https://doi.org/10.1080/03091902.2021.1891309.
[47] J.M. Johnson, D.L. Kellogg, Local thermal control of the human cutaneous circulation, J. Appl. Physiol. 109 (4) (2010) 1229–1238, https://doi.org/10.1152/japplphysiol.00407.2010.
[48] M. Sorelli, Z. Stoyneva, I.A. Mizeva, L. Bocchi, Spatial heterogeneity in the time and frequency properties of skin perfusion, Physiol. Meas. 38 (2017) 860–876, https://doi.org/10.1088/1361-6579/aa5909.
[49] C.T. Minson, Thermal provocation to evaluate microvascular reactivity in human skin, J. Appl. Physiol. 109 (2010) 1239–1246, https://doi.org/10.1152/japplphysiol.00414.2010.
[50] V.E. Brunt, C.T. Minson, Cutaneous thermal hyperemia: more than skin deep, J. Appl. Physiol. 111 (2011) 5–7, https://doi.org/10.1152/japplphysiol.00544.2011.
[51] B.J. Wong, S.M. Fieger, Transient receptor potential vanilloid type-1 (TRPV-1) channels contribute to cutaneous thermal hyperaemia in humans, J. Physiol. 588 (2010) 4317–4326, https://doi.org/10.1113/jphysiol.2010.195511.
[52] V.E. Brunt, C.T. Minson, KCa channels and epoxyeicosatrienoic acids: major contributors to thermal hyperaemia in human skin, J. Physiol. 590 (2012) 3523–3534, https://doi.org/10.1113/jphysiol.2012.236398.
[53] M. Roustit, J.-L. Cracowski, Assessment of endothelial and neurovascular function in human skin microcirculation, Trends Pharmacol. Sci. 34 (2013) 373–384, https://doi.org/10.1016/j.tips.2013.05.007.
[54] J.-L. Cracowski, C.T. Minson, M. Salvat-Melis, J.R. Halliwill, Methodological issues in the assessment of skin microvascular endothelial function in humans, Trends Pharmacol. Sci. 27 (2006) 503–508, https://doi.org/10.1016/j.tips.2006.07.008.
[55] A.A. Kamshilin, V.V. Zaytsev, A.V. Belaventseva, N.P. Podolyan, M.A. Volynsky, A. V. Sakovskaia, R.V. Romashko, O.V. Mamontov, Novel Method to Assess Endothelial Function via Monitoring of Perfusion Response to Local Heating by Imaging Photoplethysmography, Sensors 22 (2022) 5727, https://doi.org/10.3390/s22155727.
[56] Y. Matsuzawa, T. Kwon, R.J. Lennon, L.O. Lerman, A. Lerman, Prognostic Value of Flow-Mediated Vasodilation in Brachial Artery and Fingertip Artery for Cardiovascular Events: A Systematic Review and Meta-Analysis, J. Am. Heart Assoc. 4 (2015) e002270, https://doi.org/10.1161/JAHA.115.002270.
[57] O. Hahad, N. Arnold, J.H. Prochaska, M. Panova-Noeva, A. Schulz, K.J. Lackner, N. Pfeiffer, I. Schmidtmann, M. Michal, M. Beutel, P.S. Wild, J.F. Keaney, A. Daiber, T. Münzel, Cigarette Smoking Is Related to Endothelial Dysfunction of Resistance, but Not Conduit Arteries in the General Population—Results From the Gutenberg Health Study, Front. Cardiovasc. Med. 8 (2021), 674622, https://doi.org/10.3389/fcvm.2021.674622.
[58] G. Gallucci, A. Tartarone, R. Lerose, A.V. Lalinga, A.M. Capobianco, Cardiovascular risk of smoking and benefits of smoking cessation, J Thorac Dis 12 (7) (2020) 3866–3876, https://doi.org/10.21037/jtd.2020.02.47.
[59] K. Karatzi, C. Papamichael, E. Karatzis, T.G. Papaioannou, K. Stamatelopoulos, N. A. Zakopoulos, A. Zampelas, J. Lekakis, Acute smoke-induced endothelial dysfunction is more prolonged in smokers than in non-smokers, Int. J. Cardiol. 120 (2007) 404–406, https://doi.org/10.1016/j.ijcard.2006.07.200.
[60] T. Kondo, Y. Nakano, S. Adachi, T. Murohara, Effects of Tobacco Smoking on Cardiovascular Disease, Circ. J. 83 (2019) 1980–1985, https://doi.org/10.1253/circj.CJ-19-0323.
[61] H. Fushimi, M. Kubo, T. Inoue, Y. Yamada, Y. Matsuyama, M. Kameyama, Peripheral vascular reactions to smoking—profound vasoconstriction by atherosclerosis, Diabetes Res. Clin. Pract. 42 (1998) 29–34, https://doi.org/10.1016/S0168-8227(98)00084-9.
[62] E. Tur, G. Yosipovitch, S. Oren-Vulfs, Chronic and Acute Effects of Cigarette Smoking on Skin Blood Flow, Angiology 43 (1992) 328–335, https://doi.org/10.1177/000331979204300407.
[63] T.N. Meekin, R.F. Wilson, D.A. Scott, M. Ide, R.M. Palmer, Laser Doppler flowmeter measurement of relative gingival and forehead skin blood flow in light and heavy smokers during and after smoking, J. Clin. Periodontol. 27 (2000) 236–242, https://doi.org/10.1034/j.1600-051x.2000.027004236.x.
[64] K. Uehara, R. Sone, F. Yamazaki, Cigarette Smoking Following a Prolonged Mental Task Exaggerates Vasoconstriction in Glabrousa Skin in Habitual Smokers, J. UOEH. 32 (2010) 303–316, https://doi.org/10.7888/juoeh.32.303.
[65] M. Saha, V. Dremin, I. Rafailov, A. Dunaev, S. Sokolovski, E. Rafailov, Wearable Laser Doppler Flowmetry Sensor: A Feasibility Study with Smoker and Non-Smoker Volunteers, Biosensors 10 (2020) 201, https://doi.org/10.3390/bios10120201.
[66] W. Magerl, R.D. Treede, Heat-evoked vasodilatation in human hairy skin: axon reflexes due to low-level activity of nociceptive afferents, J. Physiol. 497 (1996) 837–848, https://doi.org/10.1113/jphysiol.1996.sp021814.
[67] A.A. Kamshilin, T.V. Krasnikova, M.A. Volynsky, S.V. Miridonov, O.V. Mamontov, Alterations of blood pulsations parameters in carotid basin due to body position change, Sci. Rep. 8 (2018) 13663, https://doi.org/10.1038/s41598-018-32036-7.
[68] J.M. Johnson, C.T. Minson, D.L. Kellogg Jr., Cutaneous vasodilator and vasoconstrictor mechanisms in temperature regulation, Compr. Physiol. 4 (2014) 33–89, https://doi.org/10.1002/cphy.c130015.
[69] P. Frick, I. Mizeva, S. Podtaev, Skin temperature variations as a tracer of microvessel tone, Biomed. Signal Process, Control. 21 (2015) 1–7, https://doi.org/10.1016/j.bspc.2015.04.014.
[70] P. Kvandal, S.A. Landsverk, A. Bernjak, A. Stefanovska, H.D. Kvernmo, K. A. Kirkebøen, Low-frequency oscillations of the laser Doppler perfusion signal in human skin, Microvasc. Res. 72 (2006) 120–127, https://doi.org/10.1016/j.mvr.2006.05.006.
[71] P.A. Kyriacou, S. Chatterjee, The origin of photoplethysmography, in: J. Allen, P.B. T.-P. Kyriacou (Eds.), Photoplethysmography. Technol. Signal Anal. Appl., Academic Press, 2022: pp. 17–43, https://doi.org/10.1016/B978-0-12-823374-0.00004-9.
[72] A.A. Kamshilin, E. Nippolainen, I.S. Sidorov, P.V. Vasilev, N.P. Erofeev, N. P. Podolian, R.V. Romashko, A new look at the essence of the imaging photoplethysmography, Sci. Rep. 5 (2015) 10494, https://doi.org/10.1038/srep10494.
[73] A.V. Moço, S. Stuijk, G. de Haan, New insights into the origin of remote PPG signals in visible light and infrared, Sci. Rep. 8 (2018) 8501, https://doi.org/10.1038/s41598-018-26068-2.
[74] T.Y. Abay, P.A. Kyriacou, Reflectance photoplethysmography as noninvasive monitoring of tissue blood perfusion, IEEE Trans. Biomed. Eng. 62 (2015) 2187–2195, https://doi.org/10.1109/TBME.2015.2417863.
[75] I.A. Mizeva, E.V. Potapova, V.V. Dremin, E.A. Zherebtsov, M.A. Mezentsev, V. V. Shuleptsov, A.V. Dunaev, Optical probe pressure effects on cutaneous blood flow, Clin. Hemorheol. Microcirc. 72 (2019) 259–267, https://doi.org/10.3233/CH-180459.